PROCEEDINGS of the
23rd International Congress on Acoustics

9 to 13 September 2019 in Aachen, Germany

Solution of wide-angle parabolic equations for long-range sound propagation in a moving medium

D. Keith WILSON[1]; Michael B. MUHLESTEIN[1]; Vladimir E. OSTASHEV[1]; Michael J. SHAW[1]; Michelle E. SWEARINGEN[2]; Sarah L. MCCOMAS[3]

[1] U.S. Army Engineer Research and Development Center, Hanover, NH, USA

[2] U.S. Army Engineer Research and Development Center, Champaign, IL, USA

[3] U.S. Army Engineer Research and Development Center, Vicksburg, MS, USA

ABSTRACT

Narrow-angle parabolic equations (NAPEs), which are widely used for outdoor sound propagation, are suitable for propagation angles up to 15º-20º off the nominal propagation axis (generally the horizontal direction). Wide-angle parabolic equations (WAPEs) are needed to accurately solve problems involving refraction and scattering from elevated layers at larger angles. However, it is challenging to formulate WAPEs that are numerically feasible to solve yet properly account for motion in the propagation medium, e.g., wind in the atmosphere. As a starting point, this paper considers an extra-wide-angle parabolic equation (EWAPE) for moving media which is valid for propagation angles up to 90º. Applying a Padé (1,1) approximation to the EWAPE, a new WAPE, valid for low Mach numbers and angles up to roughly 40º, is then derived. The resulting equation is generally suitable for long-range sound propagation in a windy atmosphere. As an example, calculations are given here for infrasound in the Arctic. The NAPE and WAPE solutions are compared, and the latter is found to be in better agreement with predictions for caustic locations based on ray tracing for a windy atmosphere.

Keywords: Atmosphere, Refraction, Numerical Methods

1. INTRODUCTION

Narrow-angle parabolic equations (NAPEs) are widely used to calculate the impacts of refractive gradients and ground interactions on outdoor sound propagation (1,2). They are suitable for propagation angles up to 15º-20º off the nominal propagation axis, which is typically taken to be the horizontal direction in the vertical plane of the source and receiver. NAPEs employ the effective sound-speed approximation (ESSA), in which the sound speed is replaced by the sum of the actual sound speed the component of the wind speed along the nominal axis. The ESSA can be derived as a consequence of the narrow-angle approximation (3).

Many practical long-range sound propagation problems, however, involve refraction and scattering from elevated layers which exceed the 15º-20º limitation of NAPEs. Wide-angle parabolic equations (WAPEs) are needed to accurately solve such problems (4,5,6). However, because the ESSA is not applicable at wide angles, it is challenging to formulate WAPEs that are numerically feasible to solve yet properly accounting for motion in the propagation medium.

To address the need for an accurate and computationally practical WAPE, we consider in this paper a new approach, which takes as the starting point an extra-wide-angle parabolic equation (EWAPE) for moving media (7).The EWAPE accounts for the propagation angles up to 90º with respect to the nominal propagation direction. A WAPE is then derived from the EWAPE using a Padé (1,1) approximation, which is valid for low Mach numbers and angles up to roughly 40º. Solution of this WAPE is then shown to be a straight forward extension of the conventional Crank-Nicholson method for solving the NAPE, while involving no significant additional computational burden.

We illustrate application of the new WAPE using two numerical examples for infrasound propagation, one involving a polar low and the other a katabatic wind. The NAPE and WAPE solutions are compared for these cases.

[1] d.keith.wilson@usace.army.mil

2. WAPE DERIVATION AND IMPLEMENTATION

In this section, we discuss the derivation of the WAPE and its numerical implementation. The derivation is only summarized here, as details will be provided in a future publication.

2.1 Extra wide-angle parabolic equation (EWAPE)

Our starting point is Eq. (2.88) in Ref. (3). The derivatives of the wind velocity and density appearing in this equation can be neglected at relatively high frequencies (acoustic wavelengths small compared to the size of the refractive inhomogeneities), which results in

$$\left[\frac{\partial^2}{\partial x^2}+\frac{\partial^2}{\partial \mathbf{r}^2}+k_0^2\left(1+\varepsilon+\frac{2i}{k_0 c_0}\mathbf{v}\cdot\nabla\right)\right]p(x,\mathbf{r})=0. \tag{1}$$

Here, $p(x,\mathbf{r})$ is the complex sound pressure, x is the nominal propagation direction, and $\mathbf{r}=(y,z)$ are the coordinates transverse to this direction. Furthermore, $\varepsilon=c_0^2/c^2-1$, c is the sound speed, c_0 is the reference sound speed, $k_0=2\pi f/c_0$ is the reference wavenumber, and $\mathbf{v}$ is the wind velocity.

Introducing the longitudinal and transverse Mach numbers, $M_x=v_x/c_0$ and $\mathbf{M}_\perp=\mathbf{v}_\perp/c_0$ (where $\mathbf{v}_\perp=(v_y,v_z)$ is the transverse wind), the previous result can be written

$$\left[\frac{\partial^2}{\partial x^2}+2ik_0M_x\frac{\partial}{\partial x}+k_0^2(1+\hat{\mu}+\hat{\eta})\right]p(x,\mathbf{r})=0, \tag{2}$$

where we have introduced the operators

$$\hat{\mu}=\frac{1}{k_0^2}\frac{\partial^2}{\partial \mathbf{r}^2}\quad\text{and}\quad\hat{\eta}=\varepsilon+\frac{2i}{k_0}\mathbf{M}_\perp\cdot\frac{\partial}{\partial \mathbf{r}}\ . \tag{3}$$

Factoring into waves traveling in the $+x$ and $-x$ directions, and retaining only the former, we arrive at the following one-way, pseudo-differential equation:

$$\left[\frac{\partial}{\partial x}+ik_0M_x-ik_0\sqrt{1+\hat{\mu}+\hat{\eta}}\right]p(x,\mathbf{r})=0. \tag{4}$$

For a motionless medium ($\mathbf{v}=0$), this result coincides with EWAPE2 in Ref. (7). We can regard Eq. (4) as an extension of EWAPE2 for a moving inhomogeneous medium.

2.2 Derivation of the Padé (1,1) approximation

We next approximate the pseudo-differential operator $\hat{Q}=\sqrt{1+\hat{\mu}+\hat{\eta}}$ with a Padé (n,n) series, namely

$$\hat{Q}=1+\sum_{j=1}^{n}\frac{a_{j,n}(\hat{\mu}+\hat{\eta})}{1+b_{j,n}(\hat{\mu}+\hat{\eta})}\ . \tag{5}$$

Substituting the Padé series, Eq. (5), and setting $p(x,\mathbf{r})=e^{ik_0x}\hat{p}(x,\mathbf{r})$, Eq. (4) becomes

$$\left[\frac{\partial}{\partial x}+ik_0M_x-ik_0\sum_{j=1}^{n}\frac{a_{j,n}(\hat{\mu}+\hat{\eta})}{1+b_{j,n}(\hat{\mu}+\hat{\eta})}\right]\hat{p}(x,\mathbf{r})=0. \tag{6}$$

In the remainder of this paper, we will assume that there is no transverse wind and that the derivatives in the y-direction can be neglected. (The latter approximation is typically made for PE calculations in the far field. See, for example, Ref. (2).) The operators, Eq. (3), then simplify to

$$\hat{\mu}=\frac{1}{k_0^2}\frac{\partial^2}{\partial z^2}\quad\text{and}\quad\hat{\eta}=\varepsilon\ . \tag{7}$$

We will also employ the relatively simple Padé (1,1) approximation, for which $a_{1,1}=1/2$ and $b_{1,1}=1/4$. (See Ref. (8).) Eq. (6) then becomes

$$\left[\left(\frac{\partial}{\partial x}+ik_0M_x\right)\left(1+b_{1,1}\left(\varepsilon+\frac{1}{k_0^2}\frac{\partial^2}{\partial z^2}\right)\right)-ik_0a_{1,1}\left(\varepsilon+\frac{1}{k_0^2}\frac{\partial^2}{\partial z^2}\right)\right]\hat{p}(x,z)=0. \tag{8}$$

2.3 Numerical solution

The numerical solution as presented in Ref. (3) is based on casting Eq. (8) in the form (Eq. (11.78) in

Ref. (3)):

$$\Psi_1(x,z)\frac{\partial \hat{p}}{\partial x} = ik_0\Psi_2(x,z)\hat{p}(x,z), \tag{9}$$

where $\Psi_1(x,z)$ and $\Psi_2(x,z)$ are operators with the general form

$$\Psi_m(x,z) = \sum_n h_{m,n}\left(\frac{1}{k_0}\frac{\partial}{\partial z}\right)^n.$$

Comparing Eqs. (8) and (9), we find the following non-zero values for the $h_{m,n}$:

$$h_{1,0} = 1 + b_{1,1}\varepsilon,\ h_{1,2} = b_{1,1},\ h_{2,0} = a_{1,1}\varepsilon - \left(1 + b_{1,1}\varepsilon\right)M_x,\ \text{and}\ h_{2,2} = a_{1,1} - b_{1,1}M_x. \tag{10}$$

With these values for the coefficients, numerical solution by the Crank-Nicholson method proceeds in the manner described in Sec. 11.2.2 of Ref. (3). As with the narrow-angle case (which corresponds to the preceding equations with $a_{1,1} = 1/2$ and $b_{1,1} = 0$), the Padé (1,1) formulation here involves derivatives in z up to second order, and thus entails solution of a tridiagonal matrix equation. Thus the formulation here involves only minimal modifications to existing Crank-Nicholson NAPE codes, and is just as computationally efficient.

The coefficients in Eq. (10) must be modified at the lower and upper boundaries to account for ground impedance and a radiation condition, respectively (3,9). For WAPE calculations, a wide-angle starter should also be used. The calculations in this paper employ the starter derived by Salomons (9).

3. APPLICATION TO INFRASOUND PROPAGATION IN THE ARCTIC

This section considers application of the Padé (1,1) approximation for a moving medium (Eqs. (9)-(10)) to the problem of infrasound propagation in the Arctic. This problem makes a useful and interesting test case, since refraction by temperature inversions and winds in the stratosphere generally plays a key role for infrasound propagation, and this refraction often occurs at high angles.

3.1 Weather simulation

The weather inputs for the calculations here were simulated with the polar adaptation of the Weather Research and Forecasting model, called Polar WRF (or PWRF). PWRF utilizes a polar stereographic map projection and includes sea-ice surface, ice-cloud microphysics, and other modifications to the standard WRF release (10,11) as appropriate to simulating weather at high latitudes. The PWRF simulation considered here is for the date of 6 Jan 2013 at the time 0000 UTC. The simulation has a horizontal resolution of approximately 15 km, with 34 vertical levels at pressure levels from 1000 mbar to 10 mbar. The date corresponds with the peak of a strong sudden stratospheric warming event (12), which was selected here for its likely strong influence on infrasound. The event manifests itself most notably in the stratosphere, although it evolves through time through interactions with much of the rest of the Northern Hemispheric atmosphere, impacting and being impacted by surface weather and climate phenomenon.

Two particular locations of interest were identified in the simulation based on a visual examination of the surface winds. One of these is a cyclonic disturbance in the East Siberian Sea, and the other involves a strong katabatic flow in northern Greenland. We will see that propagation predictions differ dramatically between the two locations, as might be expected owing to the especially intense gradients encountered in these cases as can often occur in the Arctic. Although the PWRF simulation provides fully 3D fields, here we have simply extracted the profiles for the two locations, and calculated the propagation under the idealization of a horizontal homogeneous atmosphere and ground surface.

3.2 Polar low in East Siberian Sea

A polar low is a small, intense cyclone forming when cold polar air is advected over warmer water. These cyclones often form in the subpolar North Pacific and subpolar North Atlantic, equatorward of the sea ice margin. Horizontal scales range from several tens to several hundreds of kilometers. Because of strong winds and intense precipitation, these cyclones are sometimes referred to as “arctic hurricanes.”

Vertical profiles were extracted from the previously described PWRF simulation at the latitude of 73.372° and longitude 150.555°, where surface analysis indicated a cyclonic wind. This location is in the East Siberian Sea. The extracted profiles are shown in Figure 1. The directions in these profiles are in the model coordinates (i.e., the PWRF polar stereographic projection), rather that Earth

coordinates. The easterly wind component exhibits jets at altitudes of about 5 km and 25 km. The northerly wind component reverses signs (from northward flow to southward flow) at an altitude of about 20 km. The temperature decreases with height through the troposphere up to 10-15 km, at which altitude the increasing temperature layer (inversion) typical of the stratosphere takes over.

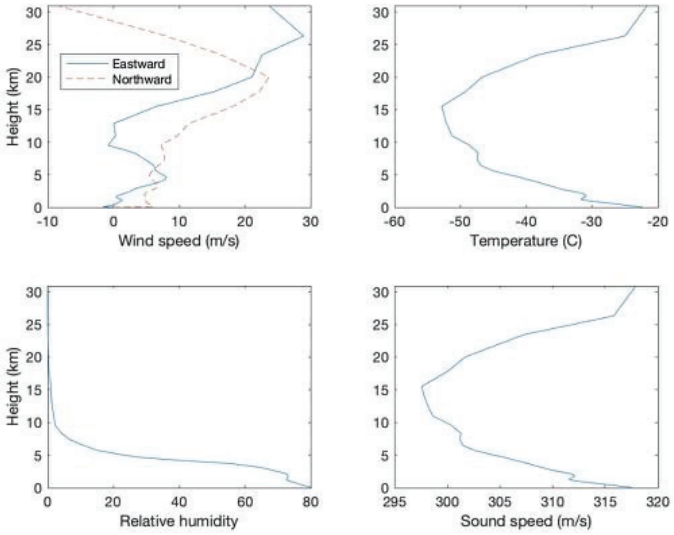

Figure 1. Vertical profiles for the East Siberian Sea, as extracted from the PWRF simulation at 0Z on 6 Jan 2013, at 73.372° latitude and 150.555° longitude. Height is km above ground (sea) level.

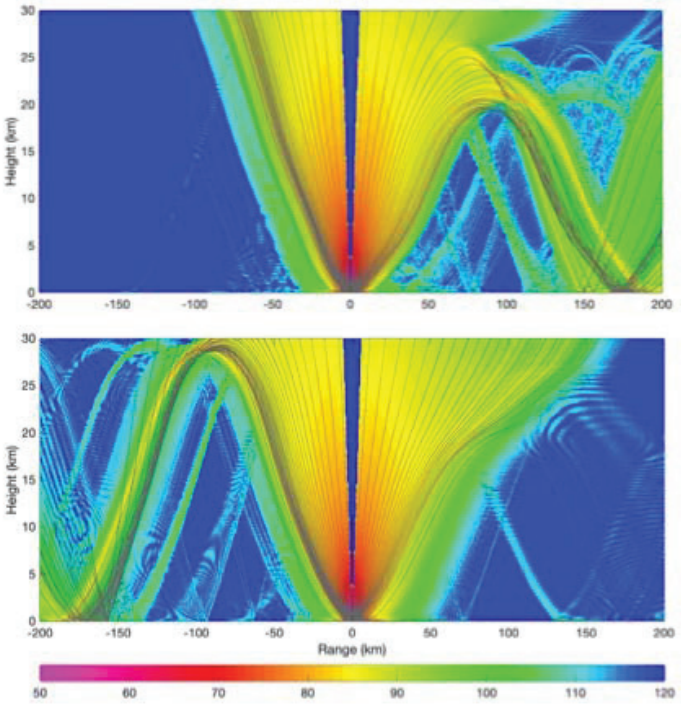

Figure 2. WAPE (Padé (1,1)) calculations for the East Siberian Sea polar low case, for a 5-Hz source at 5-m height. In the top figure, westward propagation is to the left, eastward is to the right. In the bottom figure, southward propagation is to the left, northward to the right. The color scale represents transmission loss (TL) from 50 dB to 120 dB. Gray lines are rays launched at 3° increments.

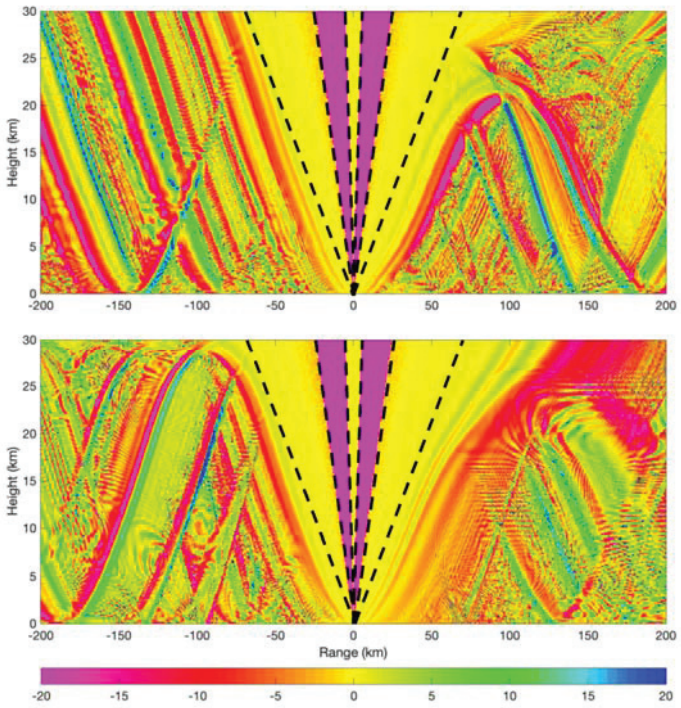

Figure 3. Similar to Figure 2, except that the difference between the WAPE and NAPE calculations is shown. The color scale represents difference in TLs on a scale from -20 dB to 20 dB. Dashed lines are shown at angles of 25°, 50°, and 80° and relative to the horizontal.

Figure 2 shows transmission loss (TL) calculations for a 5-Hz source at a height of 5 m. These calculations were made with the WAPE as derived by the Padé (1,1) approximation. A rigid ground surface was used, as is representative of water or ice. Also shown on the figure are ray paths as calculated with equations for a moving atmosphere, as described in Sec. 10.3 of Ref. (3). These equations were integrated with a Runge-Kutta method. In Figure 2, strong stratospheric returns are evident to the east and south; to the west and north, refraction is predominantly upward.

Figure 3 is similar to Figure 2, except that it shows the difference, in dB, between the WAPE calculations shown in Figure 2 and the corresponding NAPE calculations. Also shown on the plot are dashed lines at angles of 25°, 50°, and 80° and relative to the horizontal. At angles steeper than about 80°, the NAPE and WAPE are in agreement because neither has any propagating energy. At angles between 50° and 80°, the WAPE predicts lower TLs because the NAPE has no propagating energy at these angles. Interestingly, at angles between roughly 25° and 50°, the NAPE and WAPE are again in good agreement, apparently because there is minimal refraction at these angles. At angles less than about 25°, the TL difference has a very complicated behavior, probably because of multipath interference effects, for which the two approaches predict somewhat different phases in the various wave contributions.

Figure 4 shows a close-up of the propagation to the east, near the range of 100 km and altitude of 25 km. This close-up includes a well-defined caustic, i.e., a region of crossing ray paths, which indicates strong focusing of sound energy. The caustic provides a useful feature for comparing the various calculation approaches. Three different combinations of PE calculations and ray traces are compared: the NAPE with ray tracing for a moving medium, the NAPE with ray tracing based on the ESSA, and the WAPE with ray tracing for a moving medium. The WAPE appears in perfect agreement with ray tracing (for a moving medium) regarding the caustic location. The NAPE, however, misses the location of the caustic by several km. The location of the caustic agrees with the NAPE when the ESSA is employed for the ray tracing, which is to be expected since the ESSA is inherent to the NAPE. Taken together, these results provide solid evidence that the new Padé (1,1) approximation is an improvement over the NAPE and ESSA.

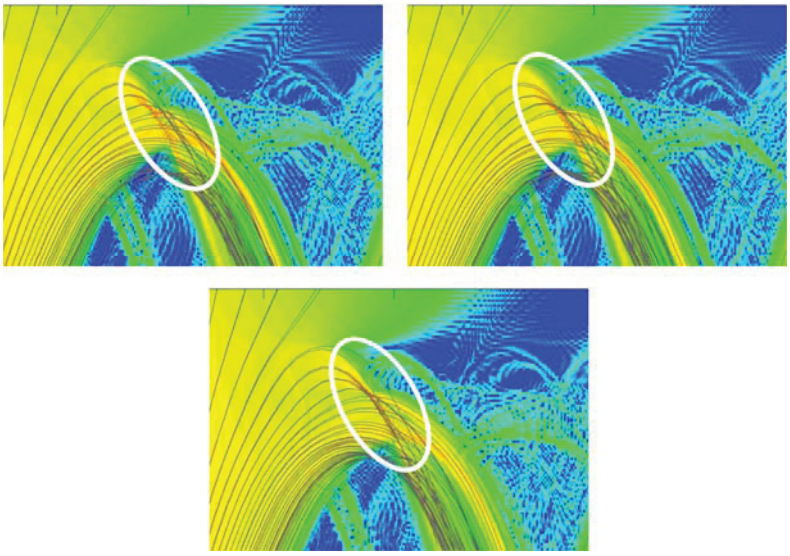

Figure 4. Close-up of the eastward propagation in the vicinity of a caustic. Top left is the NAPE calculation with rays calculated using the correct equations for a moving medium. Top right is the NAPE calculation with rays calculated using the ESSA. Bottom is the WAPE calculation with rays calculated using the correct equations for a moving medium. The location of the caustic is indicated by the white ellipses.

3.3 Katabatic wind in northern Greenland

Katabatic wind refers to any descending flow; typically, the flow consists of colder air descending on a sloped surface. Based on a visual analysis of the surface wind data from the previously mentioned PWRF simulation, a katabatic wind was evident around the latitude/longitude of (77.592°, -49.926°), and so this location was selected for more detailed analysis. The local terrain elevation is 2480 m.

The profiles for this case are shown in Figure 5. The katabatic wind is evident as a strong low-level jet, directed to the northeast, and a temperature inversion adjacent to the ground. Aloft, there is a strong westward jet at an altitude of about 20 km, and a temperature lapse prevails up to this height.

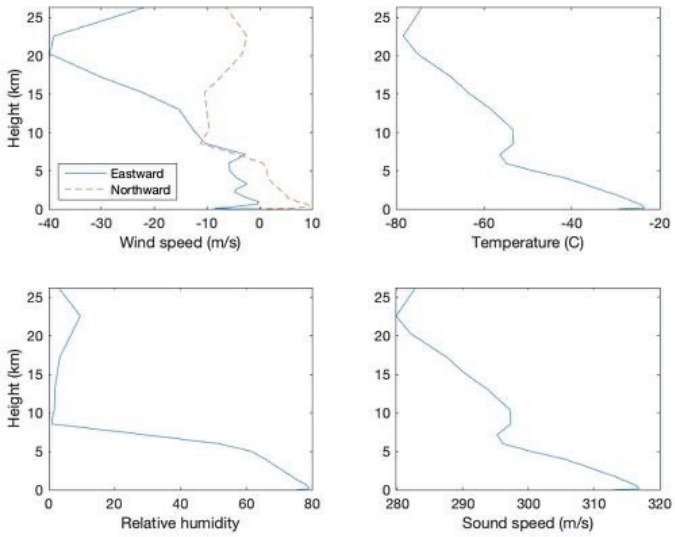

Figure 5. Vertical profiles for northern Greenland, as extracted from the PWRF simulation at 0Z on 6 Jan 2013, at 77.592° latitude and -49.926° longitude. Height is in km above ground level, which is at 2480 m.

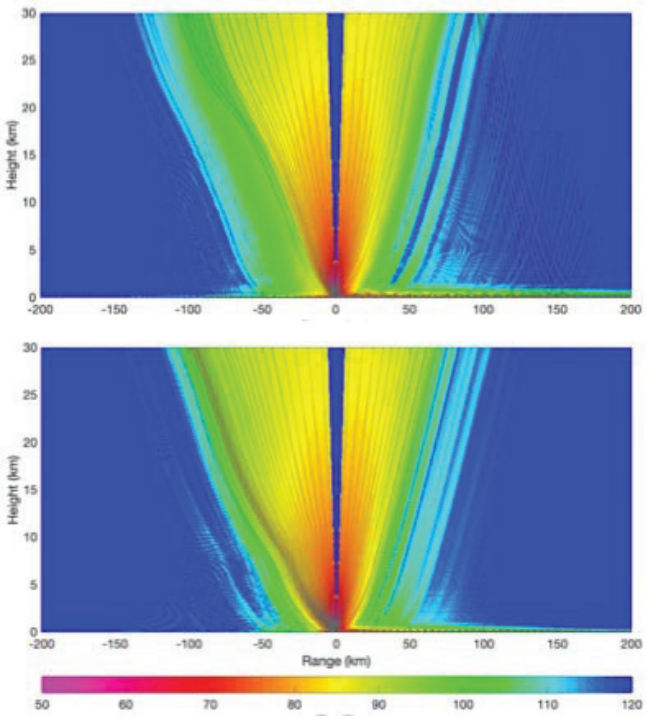

Figure 6. WAPE (Padé (1,1)) calculations for the norther Greenland katabatic wind case, for a 5-Hz source at 5-m height. See caption to Figure 2 for further explanation.

Figure 6 shows the TL calculations for a 5-Hz source at a height of 5 m, using the WAPE as derived by the Padé (1,1) approximation. A ground surface with properties characteristic of mature snow was used. Close examination of the figure reveals a surface duct at altitudes below 1 km or so, for propagation in the eastward and northward directions. This is a consequence of the katabatic wind. Above the surface duct, upward refraction prevails in all directions, due to the strong lapse rate up to a height of 20 km.

4. CONCLUSIONS

This paper presented a new wide-angle parabolic equation (WAPE) solution, which was derived from a Padé (1,1) approximation to the extra-wide angle PE (EWAPE), Eq. (4). Unlike narrow-angle parabolic equations (NAPEs), which are widely used for outdoor sound propagation and suitable for propagation angles up to 15º-20º, the new WAPE is suitable for propagation angles up to roughly 40º. Furthermore, the WAPE does not involve the effective sound speed approximation. It is valid for low Mach numbers and well suited to many applications involving refraction and scattering from elevated layers in a windy atmosphere. Conveniently, the new WAPE can be implemented with very simple changes to conventional Crank-Nicholson NAPE codes and is no more computationally intensive.

Example applications were considered here involving infrasound propagation, which provides a suitable test for wide-angle calculations due to the importance of refraction from the stratospheric temperature inversion and jet stream. PWRF was used here to model the Arctic weather. The results indicate somewhat subtle but significant differences between the NAPE and WAPE calculations. In particular, the WAPE calculations are in better agreement with ray tracing predictions for the position of a caustic in a moving atmosphere.

The PWRF calculations in this paper involved propagation around a polar low with a katabatic wind. For the polar low, some interesting interactions with the stratosphere were found, which could possibly be used to provide early warning of strong stratospheric warming events. The katabatic wind resulted in a strong low-level duct. The calculations were substantially simplified by assuming horizontal homogeneity of the atmosphere and terrain. In future research, we plan implement WAPE calculations through the full 3D fields from PWRF, including terrain elevation variations.

ACKNOWLEDGEMENTS

This research was sponsored by the U.S. Army Engineer Research and Development Center. Permission to publish was granted by Director, Cold Regions Research and Engineering Laboratory.

REFERENCES

1. Gilbert KE, White MJ. Application of the parabolic equation to sound propagation in a refracting atmosphere. J Acoust Soc Am. 1989;85(2):630-637.
2. West M, Gilbert K, Sack RA. A tutorial on the parabolic equation (PE) model used for long range sound propagation in the atmosphere. Appl Acoust. 1992;37(1):31-49.
3. Ostashev VE, Wilson DK. Acoustics in Moving Inhomogeneous Media. 2nd Ed. Boca Raton, FL, USA: CRC Press; 2015.
4. Blanc-Benon P, Dallois L, Juvé D. Long range sound propagation in a turbulent atmosphere within the parabolic approximation. Acta Acust Acust. 2001;87(6):659-669.
5. Ostashev VE, Blanc-Benon P, Juvé D, Dallois L. Wide angle parabolic equation for sound waves in a refractive, turbulent atmosphere. Proc 10th Int Symp on Long Range Sound Propagation; Grenoble, France 2002. p. 62-72.
6. Lingevitch JF, Collins MD, Dacol DK, Drob DP, Rogers JCW, Siegmann WL. A wide angle and high Mach number parabolic equation, J. Acoust Soc Am. 2002;111(2):729-734.
7. Ostashev VE, Muhlestein MB, Wilson DK. Extra-wide-angle parabolic equations in motionless and moving media, J. Acoust Soc Am. 2019;145(2) 1031-1047.
8. Collins MD. A split-step Padé solution for the parabolic equation method. J Acoust Soc Am. 1993;93(4):1736-1742.
9. Salomons E. Computational Atmospheric Acoustics, Dordrecht: Kluwer Academic; 2001.
10. Wilson AB, Bromwich DH, Hines KM. Evaluation of Polar WRF forecasts on the Arctic System Reanalysis domain: Surface and upper air analysis, J. Geophys. Res. 2011; 116, D11112.
11. Hines KM, Bromwich DH, Bai L, Bitz CM, Powers JG, Manning KW. Sea ice enhancements to Polar WRF. Monthly Weather Review 2015; 143(6) 2363-2385.
12. Coy L, Pawson S. The major stratospheric sudden warming of January 2013: Analyses and forecasts in the GEOS-5 data assimilation system. Monthly Weather Review 2015; 143(2) 491-510.